PAH growth in flames and space: phenalenyl radical from acenaphthylene

Zachariah D. Levey,[†] Benjamin A. Laws,[†] Klaas Nauta,[†] Scott H. Kable,[†] Gabriel da Silva,[‡] John F. Stanton,[¶] and Timothy W. Schmidt[*,§]

†*School of Chemistry, University of New South Wales, Sydney NSW 2052, Australia*

‡*Department of Chemical Engineering, The University of Melbourne, Parkville 3XXX, Australia*

¶*Department of Chemistry, University of Florida, Gainesville, Florida 32611, USA*

§*Centre of Excellence in Exciton Science, University of New South Wales, Sydney NSW 2052, Australia*

E-mail: timothy.schmidt@unsw.edu.au

Abstract

Polycyclic aromatic hydrocarbons (PAHs) are intermediates in the formation of soot particles and interstellar grains. However, their formation mechanisms in combustion and interstellar environments are not fully understood. The production of tricyclic PAHs and, in particular, the conversion of a PAH containing a five-membered ring to a six-membered ring is of interest to explain PAH abundances in combustion processes. In the present work, resonant ionization mass spectrometry in conjunction with isotopic labelling is used to investigate the formation of the phenalenyl radical from acenaphthylene and methane in an electrical discharge. We show that in this environment, the CH cycloaddition mechanism converts a five-membered ring to a six-membered ring. This mechanism can occur in tandem with other PAH formation mechanisms such as

hydrogen abstraction/ acetylene addition (HACA) to produce larger PAHs in flames and the interstellar medium.

Introduction

Polycyclic aromatic hydrocarbons (PAHs) are early intermediates in the soot formation process in both terrestial[1–3] and interstellar environments.[4–7] Soot and PAHs formed during the incomplete combustion of fossil fuels are detrimental to human health due to their toxic and carcinogenic properties.[8–11] A ubiquitous existence of PAHs in the interstellar medium (ISM) is inferred from the aromatic infrared bands (AIBs), a set of infrared emission features between $3 - 20\,\mu$m that are characteristic of large PAH molecules.[12,13] It is thought that PAHs may comprise up to 20% of the total cosmic carbon abundance.[14–16] Benzene and benzonitrile, as well as fullerenes have been identified in the ISM.[17–20] However, the detection of any specific PAH had been elusive, until recently, when the emission from 1- and 2-cyanonaphthalene was observed within the Taurus Molecular Cloud, TMC-1 (mcg21).

The formation mechanism for interstellar PAHs is ambiguous. Astrochemical models of PAH formation are derived from combustion chemistry models.[21] Bottom-up molecular growth processes in circumstellar envelopes of carbon-rich stars are largely based on the hydrogen abstraction-acetylene addition (HACA) mechanism.[12] HACA proceeds by activation of a radical site by H-abstraction or addition followed by addition of acetylene and ring closure.[22] It has been shown to occur for the formation of naphthalene from benzene via a phenylacetylene intermediate,[23,24] as well as for the formation of pyrene from 4-phenanthrenyl radical.[25]

However, there are some shortcomings of the HACA mechanism. Notably, modelling studies have reported that HACA under-predicts the concentration of PAHs in flames,[26] and under-predicts the PAH growth rate in astrochemical models.[27–29] To address these deficiencies, additional PAH formation mechanisms have been proposed. These include:

recombination of resonance-stabilized radicals;[30–32] dimerization of small PAHs;[33] phenyl addition/cyclization;[34] methyl addition/cyclization,[35] and methylidyne addition-cyclization-aromatization (MACA) dod21.

Acenaphthylene (ACYN) is considered the first significant island of stability pulling the HACA sequence forward.[36] Theoretical investigations of the reaction between naphthalene and acetylene show predominant formation of ACYN over phenanthrene and anthracene. Rapid cyclization after the addition of a single acetylene adjacent to the bay region to form a five-membered ring occurs faster than the addition of a second acetylene, followed by cyclization to form a third aromatic ring.[37] Indeed, three-quarters of the PAH products of the reaction contain a five-membered ring and less than 6% are PAHs with exclusively six-membered rings.[37] Hence, a mechanism to convert a five-membered ring on the edge of a PAH to a six-membered ring is necessary to account for pathways to larger PAHs.

Ring expansion has been proposed to take place by methylation followed by rearrangement and H-loss, and this mechanism has been invoked to account for benzene formation from cyclopentadienyl radical and naphthalene formation from indene.[30,38–43] Recently, calculations for the reaction of 1-acenaphthyl and methyl suggest that ring expansion of the five-membered ring occurs by methylation to produce 1H-phenalene and the phenalenyl radical.[44] The phenalenyl radical[45,46] is posited to have a role in soot inception and growth.[32] It consists of three aromatic rings which share a central carbon atom. The gas phase excitation spectrum for the $D_1 \leftarrow D_0$ electronic transition was reported by our group.[47]

Additionally, expansion of a five-membered ring to a six-membered ring has been demonstrated through the reaction of pyrrole with the methylidyne radical (CH) to form pyridine,[48] and the reaction of cyclopentadiene with CH to form benzene.[49] CH in its ground state has been detected in combustion environments,[50–52] the interstellar medium[53,54] and under plasma conditions.[55] Reactions between CH and small unsaturated hydrocarbons and carbonyls can result in CH insertion to a π-bond through a cyclic intermediate (cycloaddition) followed by ring-opening.[49,56–59] This reaction has a negligible activation barrier, resulting in fast reaction rates. Isotopomer distribution experiments provide additional evidence for this mechanism through the reaction of CD with ethylene and pyrrole.[48,56] CH is incorporated in the MACA mechanism, which has been demonstrated through the formation of indene from styrene. Our group has also reported the formation of the methyltropyl radical from the discharge of toluene, an example of a six-membered ring converting to a seven-membered ring through CH insertion (rei18).

In an electrical discharge containing methane, both methyl radicals and CH will be present. Introducing ACYN thus allows the CH insertion reaction to compete with the methylation ring expansion reaction to generate phenalenyl radicals. But, these mechanisms will incorporate a different number of deuterium atoms if CH_4 is substituted with CD_4. In this work, we investigated the products of an electrical discharge containing methane and ACYN. We identified phenalenyl radical ($C_{13}H_9$) as a product, and with perdeuterated methane detected a $C_{13}H_8D$ radical identified to be d1-phenalenyl. No $C_{13}H_7D_2$ radical was observed, which is strong evidence for CH cycloaddition as the dominant ring expansion mechanism. We propose that this reaction occurs in partnership with HACA to overcome the acenaphthylene bottleneck and lead to the generation of large PAHs.

Results and Discussion

The mass spectrum of an ACYN-containing argon beam (1% CH_4/ 99% Ar, Coregas) ionized by a 266 nm laser pulse is shown in Fig. 1(a). At this wavelength, species with an $IE < 9.32$ eV may be ionized through (resonant) 2-photon ionization (R2PI). The ACYN parent signal (m/z 152) is minor compared to m/z 154. The m/z 154 signal corresponds to acenaphthene (ACN), an impurity in the sample, that is resonance-enhanced at 266 nm ($S_2 \leftarrow S_0$ electronic transition).[60] Peaks at m/z 153 and m/z 155 are assigned to hydrogen atom loss and the ^{13}C isotopologue of ACN, respectively. The species at m/z 172 is unidentified.

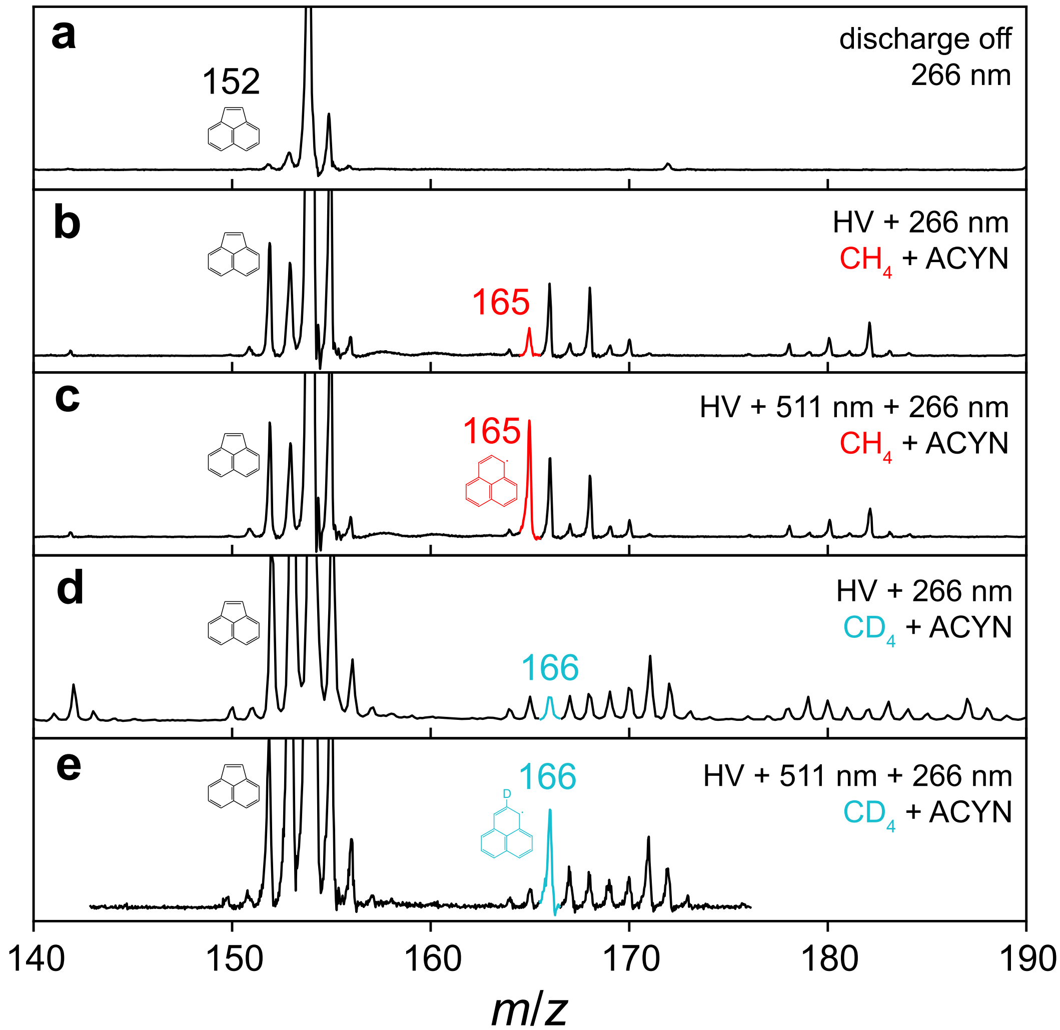

Figure 1: Mass spectra of products formed in high voltage (HV) electric discharge containing acenaphthylene and CH_4/CD_4. a) R2PI of ACYN at 266 nm without electric discharge. b) R2PI of products formed in electric discharge from ACYN + CH_4 at 266 nm. c) R2C2PI of products formed in electrical discharge from ACYN + CH_4. Excitation laser tuned to transition of phenalenyl at 19560 cm^{-1} (511 nm) and preceding ionisation laser at 266 nm by 30 ns. The phenalenyl radical (m/z 165) is highlighted in red. d) R2PI of products formed in electric discharge from ACYN + CD_4 at 266 nm. e) R2C2PI of products formed in electrical discharge from ACYN + CD_4. Excitation laser tuned to transition at 19565 cm^{-1} and preceding ionisation laser at 266 nm by 30 ns. The phenalenyl radical (m/z 165) is highlighted in cyan.

Figure 1(b) shows the mass spectrum from ACYN, with a high voltage (HV) discharge of -1.05 kV striking the molecular beam expansion 2 cm after the pulsed nozzle. Two new groups of ions are generated by the HV discharge between m/z 164 – 170 and m/z 178 –

184, respectively. These two groups are subsequently spaced from the parent signal (m/z 152) by 12 – 18 amu indicating the consecutive addition of CH_n, where $n = 0 - 6$.

The species at m/z 165 is assigned to the phenalenyl radical, $C_{13}H_9$, resulting from net CH addition to ACYN. The peak at m/z 166 is assigned to 1H-phenalene, $C_{13}H_{10}$.[46] The other significant ion signal in this cluster is at m/z 168, which corresponds to the addition of CH_4 to ACYN, resulting in a molecular formula of $C_{13}H_{12}$. A likely suspect is a species similar to 1H-phenalene but with three individual, peripheral, sp^3 carbons. Additional minor peaks at m/z 167 and 169 are most likely a combination of ^{13}C isotopologues (of m/z 166 and 168) and radical species.

To confirm the assignment of m/z 165, a tunable laser pulse was introduced to excite the radicals, preceding the ionizing laser pulse by ∼30 ns. The wavelength of the excitation laser was scanned from $541 - 476$ nm to measure the R2C2PI spectrum for the $D_1 \leftarrow D_0$ transition of the phenalenyl radical. Figure 2 shows a comparison with the R2C2PI spectrum recorded by O'Connor et al.[47] The resonance-enhanced ion signal resulting from the excitation laser being tuned to the wavelength of the strongest vibronic transition is shown in Fig. 1(c).

The formation mechanism of the phenalenyl radical from ACYN was investigated by substituting perdeuterated methane, CD_4, into the seeding gas mixture. The resultant mass spectrum from 266 nm ionization is shown in Fig. 1(d). As with the non-deuterated mass spectrum, there are two distinct mass peak clusters produced by CD_n and C_2D_n addition to ACYN and ACN.

The wavelength of the excitation laser was scanned around 511 nm to maximize the m/z 166 signal. The resultant mass spectrum is displayed in Fig. 1(e). The resonance enhancement strongly suggests that the m/z 166 mass signal corresponds to the d1-phenalenyl radical, $C_{13}H_8D$.

To confirm this assignment, the excitation laser was scanned from 535 nm to 475 nm. A comparison between the R2C2PI spectra of the phenalenyl radical and the species with m/z 166 is shown in Fig. 3. Importantly, no other species produced a vibronic spectrum in this

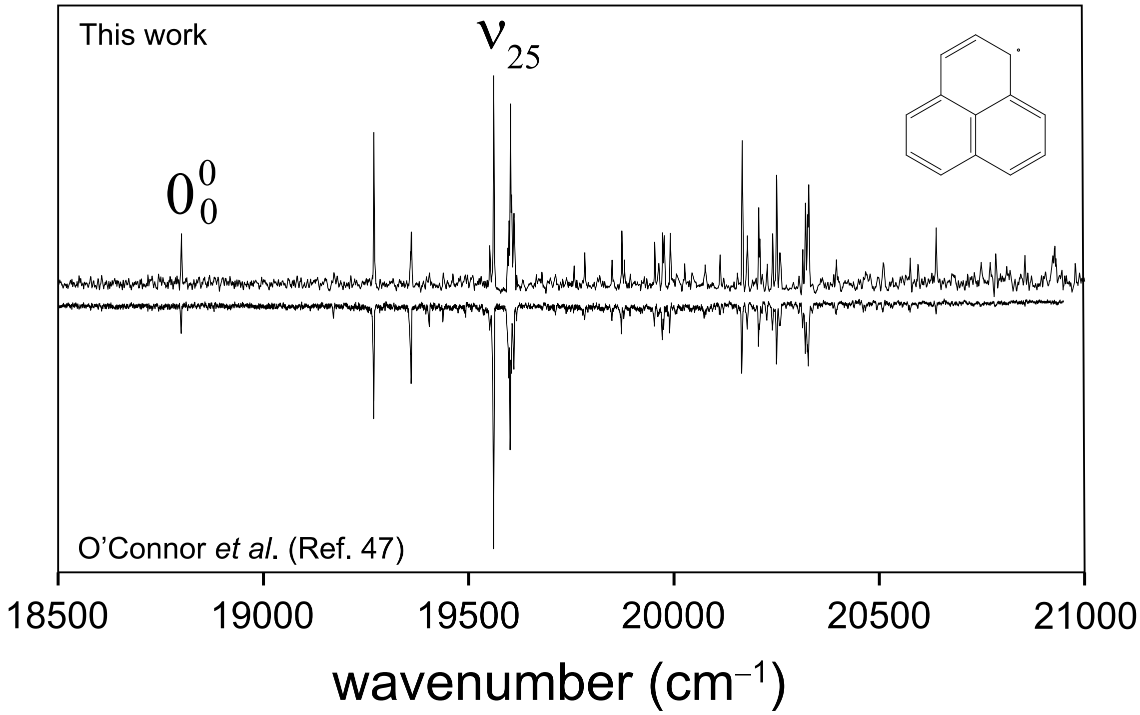

Figure 2: Resonant ionisation spectra of the phenalenyl radical (m/z 165). Top panel: R2C2PI spectrum recorded in this work (black). Bottom panel: R2C2PI spectrum recorded by O'Connor *et al.*[47] (blue).

wavelength range. The strong resemblance to the spectrum of the phenalenyl radical confirms the assignment of m/z 166 to $C_{13}H_8D$. Each peak (cluster) in the deuterated spectrum has been shifted to higher energy by $\sim 5\,\mathrm{cm}^{-1}$ compared to the original spectrum.

It may be tempting to ascribe the splitting of the origin peak at 18800 cm^{-1} to two different deuteration sites: either on or off the C_2 axes. However, the D_1 state of phenalenyl is a $E'' \otimes e'$ Jahn-Teller problem. Briefly, the potential energy part of the Hamiltonian for the $1E''$ state of phenalenyl can be written, in the diabatic basis,

$$\mathbf{V} = \begin{bmatrix} \lambda\rho^2 - kQ_x + (\delta Q_x) & +kQ_y \\ +kQ_y & \lambda\rho^2 + kQ_x \end{bmatrix} \tag{1}$$

where the rows and columns represent the two components of the degenerate electronic state, $|\mathcal{E}_x\rangle, |\mathcal{E}_y\rangle$. The symbols Q_x and Q_y are the components of a degenerate e' Jahn-Teller active mode, with $\rho^2 = Q_x^2 + Q_y^2$. The term in parentheses is discussed below. Diagonalization of this matrix ($\delta = 0$) generates the familiar Jahn-Teller conical intersection.

With a single deuterium atom in the 2-position (C_{2v}), there will be a zero-point energy difference between positive and negative distortions in, say, Q_x. This is quantum-induced symmetry-breaking, as observed in dihydroanthracenyl radicals.[61] This effect is introduced by augmenting the linear term in at least one of the diagonal matrix elements. This tilts the potential to localize the minimum energy.[62] A full account of this effect in asymmetrically deuterated cyclopentadienyl radicals is given in Reference 62.

In the basis of $|\mathcal{E}_{x,y}\rangle \otimes |v_x, v_y\rangle$ harmonic oscillator wavefunctions, $|\mathcal{E}_{x,y}\rangle \otimes \{|0,0\rangle, |0,1\rangle, |1,0\rangle\}$ which are eigenfunctions of the potential $V = \lambda\rho^2$, with eigenvalues $\{\epsilon_0, \epsilon_1, \epsilon_1\}$

$$\mathbf{H} = \begin{bmatrix} \epsilon_0 & -k' & 0 & 0 & 0 & +k \\ -k' & \epsilon_1 & 0 & 0 & 0 & 0 \\ 0 & 0 & \epsilon_1 & +k & 0 & 0 \\ 0 & 0 & +k & \epsilon_0 & +k & 0 \\ 0 & 0 & 0 & +k & \epsilon_1 & 0 \\ +k & 0 & 0 & 0 & 0 & \epsilon_1 \end{bmatrix} \tag{2}$$

where $\langle 1|Q_{x,y}|0\rangle = 1$ and $k' = k - \delta$. In the absence of zero-point energy effects, diagonalization of this matrix yields a degenerate ground state. However, the term δ lifts this degeneracy, resulting in the splitting observed in Figure 3. An even more complicated pattern than is observed might be expected were there both isotopomers present, in addition to the asymmetric Jahn-Teller effect. A complete assignment of the deuterated spectrum will be provided in a forthcoming publication.

This result provides insight into the formation mechanism of phenalenyl radical from ACYN. A mass shift from m/z 165 to 166 suggests that only a single deuterium atom has been substituted into the phenalenyl radical. This is inconsistent with the methylation mechanism put forth by Porfiriev *et. al.*,[44] in which hydrogen abstraction from ACYN allows for

CH_3 (CD_3) addition to the resultant radical site of the acenaphthyl radical. The methylated product may then follow several different pathways leading to the phenalenyl radical. However, each pathway in this proposed reaction scheme involves two hydrogen (deuterium) atoms from the CH_3 (CD_3) radical being present in the final product.[44] The deuterated reaction scheme for the methylation mechanism is shown in Fig. 4a.

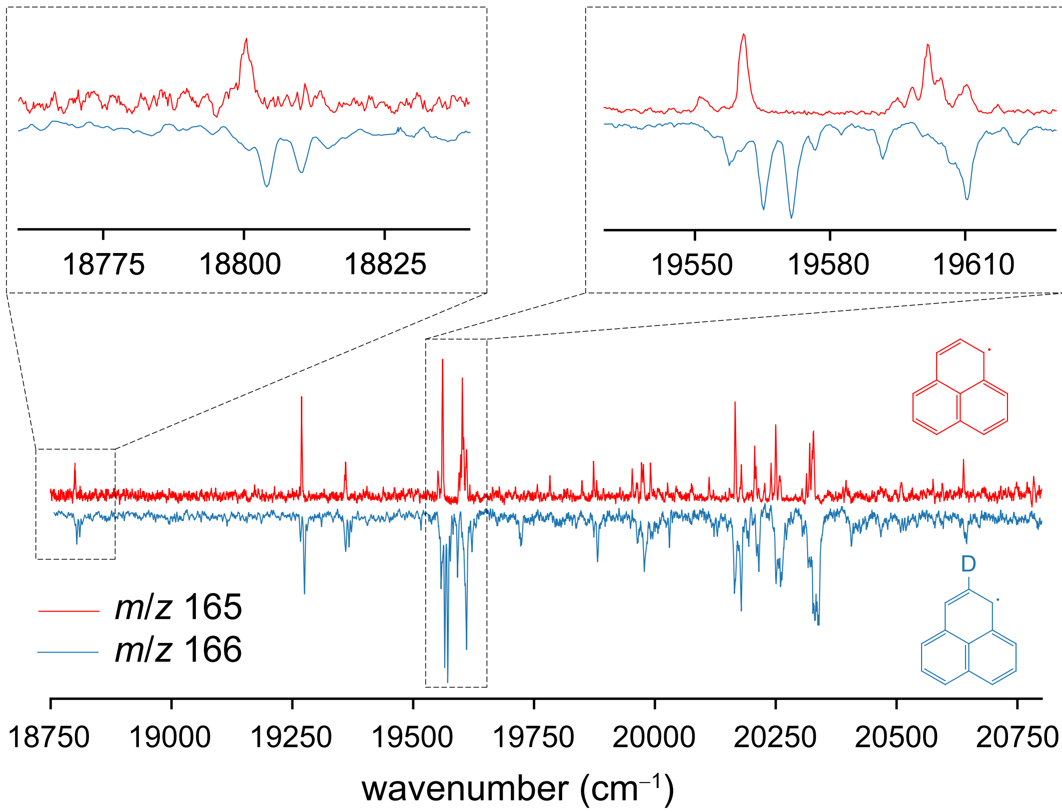

Figure 3: Top: A comparison of the resonant ionisation spectra of phenalenyl radical ($C_{13}H_9$) (red) and deuterated phenalenyl radical ($C_{13}H_8D$) (blue). Top left: Origin band. Top right: Most intense bands in the spectrum.

Results from this work are in agreement with the CH cycloaddition mechanism reported by Trevitt and Goulay.[59] Figure 4b displays the presently hypothesized reaction mechanism for the formation of phenalenyl radical from ACYN. In this reaction, the CH or CD radical is inserted across the π-bond of the cyclopenta-fused ring of ACYN, forming a bicyclic intermediate. This may then isomerize, resulting in ring opening and the formation of the third six-membered ring. For this scheme, there is no abstraction of the original hydrogens of

ACYN and only a single additional hydrogen/deuterium is required to form the phenalenyl radical.

Will then discuss the computational results by Gabe

The CH cycloaddition mechanism working in conjunction with the HACA mechanism is a plausible explanation for the production of the multitude of large, planar PAHs formed in combustion processes. The HACA mechanism will predominantly generate a five-membered ring in the bay region of a PAH. The CH cycloaddition mechanism will then cause ring expansion to form another six-membered ring, and the process can repeat itself. This subsequent combination of mechanisms can account for the formation of PAHs beyond the phenalenyl radical, such as pyrene, cyclopenta[cd]pyrene and the olympicenyl radical. The high concentrations of CH radicals in combustion environments and its detection in the interstellar medium further supports the plausibility of CH cycloaddition as a crucial component of the PAH formation mechanism.[50–54]

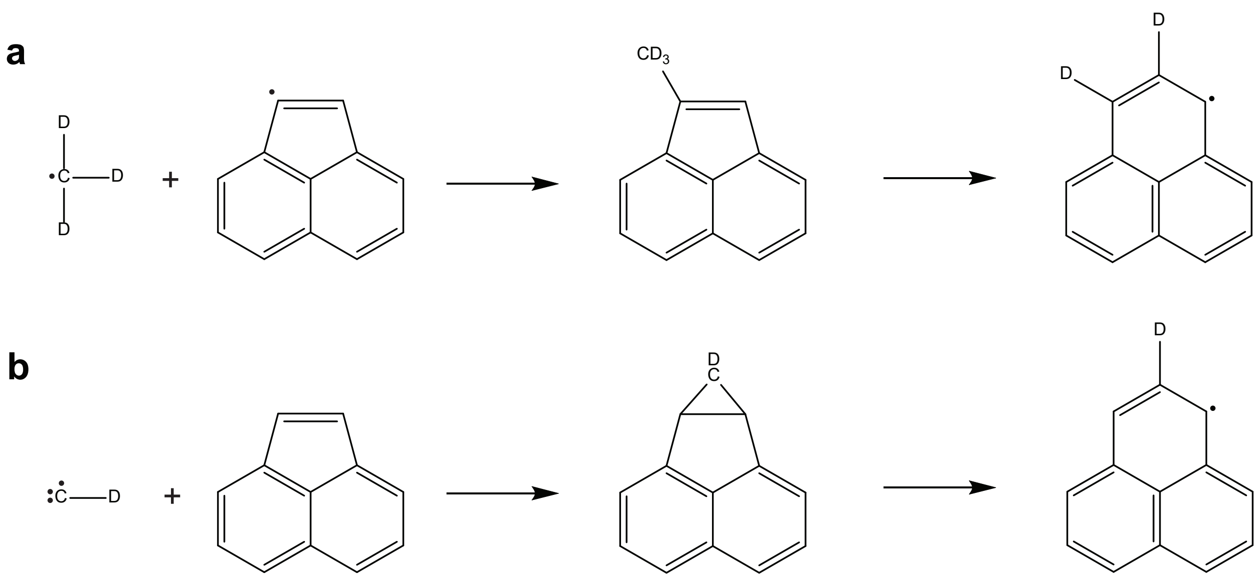

Figure 4: a) Methylation reaction scheme for formation of phenalenyl radical from 1-acenaphthyl radical + $CD_3\cdot$, proposed by Porfiriev *et. al.*[44] b) Cycloaddition reaction scheme for the formation of phenalenyl radical from acenaphthylene + $CD\cdot$.

Conclusion

We have shown that the phenalenyl radical is produced as a discharge product of ACYN and methane. Substituting CD_4 into the seeding gas mixture indicated that the dominant formation mechanism was CH cycloaddition. This reaction occurs through the insertion of CH across the C−C π-bond of the cyclopenta-fused ring of ACYN, forming a three-membered ring, followed by ring-opening to generate the phenalenyl radical. This contradicts the suggestion that the reaction occurs by methylation.[44] The conversion of ACYN to the phenalenyl radical is an example of a five-membered ring expanding to a six-membered ring, which is of importance in combustion and interstellar chemistry, and the abundance of CH supports the proposed mechanism in these environments. The CH cycloaddition mechanism may work in tandem with the HACA mechanism to generate larger PAHs beyond the tricyclic phenalenyl radical.

Experimental Details

The apparatus used for R2C2PI and R2PI has been described previously in more detail.[63] A sample of ACYN is heated to 85°C and seeded in 5 bar of a methane/argon gas mixture(Coregas, 1% Methane/99% Argon). The seeded gas mix is expanded into a differentially pumped vacuum chamber through a pulsed discharge nozzle (PDN). A voltage of −1.05kV is applied to the outer electrode of the PDN for 100 μs, resulting in a strike which coincides with the expanding gas pulse.

Methane is incorporated into the backing gas mixture to provide an additional source of CH. The discharge products are cooled through supersonic expansion and the central, coldest section of the molecular beam (∼10K) is passed through a 2 mm diameter skimmer into a second differentially pumped chamber. The cold molecular beam is probed between two positively charged extraction plates of a Wiley-McLaren-type time-of-flight mass spectrometer (ToF-MS) using R2C2PI spectroscopy.

A Nd:YAG-pumped dye laser is used as an excitation laser to investigate the first electronic excited states of the phenalenyl radical. The excited radicals are subsequently ionized using the fourth harmonic (266 nm) of a second Nd:YAG laser, pulsing a few tens of nanoseconds after the excitation pulse. The resultant cations are orthogonally accelerated up the length of the ToF-MS and detected by a multichannel plate (MCP) which produces an electronic signal that is displayed on an oscilloscope. Custom-written LabView software is used to record the spectra and a wavemeter is used to calibrate the laser wavelengths.

Acknowledgement

This research was funded by the Australian Research Council (DP190103151). TWS is supported by the Australian Research Council Centre of Excellence in Exciton Science (CE170100026).

References

(1) Frenklach, M. Reaction mechanism of soot formation in flames. *Phys. Chem. Chem. Phys.* **2002**, *4*, 2028–2037.

(2) Wang, H. Formation of nascent soot and other condensed-phase materials in flames. *P. Combust. Inst.* **2011**, *33*, 41 – 67.

(3) Faccinetto, A.; Irimiea, C.; Minutolo, P.; Commodo, M.; D'Anna, A.; Nuns, N.; Carpentier, Y.; Pirim, C.; Desgroux, P.; Focsa, C.; et al., Evidence on the formation of dimers of polycyclic aromatic hydrocarbons in a laminar diffusion flame. *Commun. Chem.* **2020**, *3*, 112.

(4) Henning, T.; Salama, F. Carbon in the Universe. *Science* **1998**, *282*, 2204–2210.

(5) Jäger, C.; Huisken, F.; Mutschke, H.; Jansa, I. L.; Henning, T. Formation of Polycyclic Aromatic Hydrocarbons and Carbonaceous Solids in Gas-Phase Condensation Experiments. *Astrophys. J.* **2009**, *696*, 706–712.

(6) Draine, B. T.; Li, A. Infrared Emission from Interstellar Dust. I. Stochastic Heating of Small Grains. *Astrophys. J.* **2001**, *551*, 807–824.

(7) Draine, B. T.; Li, A. Infrared Emission from Interstellar Dust. IV. The Silicate-Graphite-PAH Model in the Post-Spitzer Era. *Astrophys. J.* **2007**, *657*, 810–837.

(8) Ramanathan, V.; Carmichael, G. Global and regional climate changes due to black carbon. *Nat. Geosci.* **2008**, *1*, 221–227.

(9) Finlayson-Pitts, B. J. Tropospheric Air Pollution: Ozone, Airborne Toxics, Polycyclic Aromatic Hydrocarbons, and Particles. *Science* **1997**, *276*, 1045–1051.

(10) Denissenko, M. F.; Pao, A.; Tang, M.-S.; Pfeifer, G. P. Preferential Formation of Benzo[a]pyrene Adducts at Lung Cancer Mutational Hotspots in P53. *Science* **1996**, *274*, 430–432.

(11) Tiwari, M.; Sahu, S.; Pandit, G. Distribution of PAHs in different compartment of creek ecosystem: Ecotoxicological concern and human health risk. *Environ. Toxicol. Phar.* **2017**, *50*, 58 – 66.

(12) Tielens, A. G. G. M. The molecular universe. *Rev. Mod. Phys.* **2013**, *85*, 1021–1081.

(13) Pech, C.; Joblin, C.; Boissel, P. The profiles of the aromatic infrared bands explained with molecular carriers. *Astron. Astrophys.* **2002**, *388*, 639–651.

(14) Tielens, A. Interstellar Polycyclic Aromatic Hydrocarbon Molecules. *Annu. Rev. Astron. Astr.* **2008**, *46*, 289–337.

(15) Dwek, E.; Arendt, R. G.; Fixsen, D. J.; Sodroski, T. J.; Odegard, N.; Weiland, J. L.; Reach, W. T.; Hauser, M. G.; Kelsall, T.; Moseley, S. H.; et al., Detection and Characterization of Cold Interstellar Dust and Polycyclic Aromatic Hydrocarbon Emission, from COBE Observations. *Astrophys. J.* **1997**, *475*, 565–579.

(16) D'Hendecourt, L.; Ehrenfreund, P. Spectroscopic properties of polycyclic aromatic hydrocarbons (PAHs) and astrophysical implications. *Adv. Space Res.* **1997**, *19*, 1023–1032.

(17) Cernicharo, J.; Heras, A. M.; Tielens, A. G. G. M.; Pardo, J. R.; Herpin, F.; Guélin, M.; Waters, L. B. F. M. *Infrared Space Observatory's* Discovery of C_4H_2, C_6H_2, and Benzene in CRL 618. *Astrophys. J.* **2001**, *546*, L123–L126.

(18) McGuire, B. A.; Burkhardt, A. M.; Kalenskii, S.; Shingledecker, C. N.; Remijan, A. J.; Herbst, E.; McCarthy, M. C. Detection of the aromatic molecule benzonitrile (c-C_6H_5CN) in the interstellar medium. *Science* **2018**, *359*, 202–205.

(19) Cami, J.; Bernard-Salas, J.; Peeters, E.; Malek, S. E. Detection of C_{60} and C_{70} in a Young Planetary Nebula. *Science* **2010**, *329*, 1180–1182.

(20) Campbell, E. K.; Holz, M.; Gerlich, D.; Maier, J. P. Laboratory confirmation of C_{60}^+ as the carrier of two diffuse interstellar bands. *Nature* **2015**, *523*, 322–323.

(21) Frenklach, M.; Feigelson, E. D. Formation of Polycyclic Aromatic Hydrocarbons in Circumstellar Envelopes. *Astrophys. J.* **1989**, *341*, 372.

(22) Frenklach, M.; Clary, D. W.; Gardiner, W. C.; Stein, S. E. Detailed kinetic modeling of soot formation in shock-tube pyrolysis of acetylene. *Symp. (Int.) Combust.* **1985**, *20*, 887 – 901.

(23) Parker, D. S. N.; Kaiser, R. I.; Troy, T. P.; Ahmed, M. Hydrogen Abstraction/Acetylene Addition Revealed. *Angew. Chem. Int. Edit.* **2014**, *53*, 7740–7744.

(24) Yang, T.; Troy, T. P.; Xu, B.; Kostko, O.; Ahmed, M.; Mebel, A. M.; Kaiser, R. I. Hydrogen-Abstraction/Acetylene-Addition Exposed. *Angew. Chem. Int. Edit.* **2016**, *55*, 14983–14987.

(25) Zhao, L.; Kaiser, R. I.; Xu, B.; Ablikim, U.; Ahmed, M.; Joshi, D.; Veber, G.; Fischer, F. R.; Mebel, A. M. Pyrene synthesis in circumstellar envelopes and its role in the formation of 2D nanostructures. *Nat. Astron.* **2018**, *2*, 413–419.

(26) Raj, A.; Prada, I. D. C.; Amer, A. A.; Chung, S. H. A reaction mechanism for gasoline surrogate fuels for large polycyclic aromatic hydrocarbons. *Combust. Flame* **2012**, *159*, 500 – 515.

(27) Micelotta, E. R.,; Jones, A. P.,; Tielens, A. G. G. M., Polycyclic aromatic hydrocarbon processing in a hot gas. *Astron. Astrophys.* **2010**, *510*, A37.

(28) Micelotta, E. R.,; Jones, A. P.,; Tielens, A. G. G. M., Polycyclic aromatic hydrocarbon processing in interstellar shocks. *Astron. Astrophys.* **2010**, *510*, A36.

(29) Micelotta, E. R.,; Jones, A. P.,; Tielens, A. G. G. M., Polycyclic aromatic hydrocarbon processing by cosmic rays. *Astron. Astrophys.* **2011**, *526*, A52.

(30) Melius, C. F.; Colvin, M. E.; Marinov, N. M.; Pit, W. J.; Senkan, S. M. Reaction mechanisms in aromatic hydrocarbon formation involving the C_5H_5 cyclopentadienyl moiety. *Symp. (Int.) Combust.* **1996**, *26*, 685 – 692.

(31) Miller, J. A.; Melius, C. F. Kinetic and thermodynamic issues in the formation of aromatic compounds in flames of aliphatic fuels. *Combust. Flame* **1992**, *91*, 21 – 39.

(32) Johansson, K. O.; Head-Gordon, M. P.; Schrader, P. E.; Wilson, K. R.; Michelsen, H. A. Resonance-stabilized hydrocarbon-radical chain reactions may explain soot inception and growth. *Science* **2018**, *361*, 997–1000.

(33) Siegmann, K.; Sattler, K. Formation mechanism for polycyclic aromatic hydrocarbons in methane flames. *J. Chem. Phys.* **2000**, *112*, 698–709.

(34) Shukla, B.; Susa, A.; Miyoshi, A.; Koshi, M. Role of Phenyl Radicals in the Growth of Polycyclic Aromatic Hydrocarbons. *J. Phys. Chem. A* **2008**, *112*, 2362–2369, PMID: 18298104.

(35) Shukla, B.; Miyoshi, A.; Koshi, M. Role of Methyl Radicals in the Growth of PAHs. *J. Am. Soc. Mass Spectr.* **2010**, *21*, 534 – 544.

(36) Frenklach, M.; Mebel, A. M. On the mechanism of soot nucleation. *Phys. Chem. Chem. Phys.* **2020**, *22*, 5314–5331.

(37) Kislov, V. V.; Sadovnikov, A. I.; Mebel, A. M. Formation Mechanism of Polycyclic Aromatic Hydrocarbons beyond the Second Aromatic Ring. *J. Phys. Chem. A* **2013**, *117*, 4794–4816, PMID: 23672431.

(38) Moskaleva, L.; Mebel, A.; Lin, M. The CH_3+C_5H_5 reaction: A potential source of benzene at high temperatures. *Symp. (Int.) Combust.* **1996**, *26*, 521 – 526.

(39) Sharma, S.; Green, W. H. Computed Rate Coefficients and Product Yields for c-C_5H_5 + CH_3 $\rightarrow$ Products. *J. Phys. Chem. A* **2009**, *113*, 8871–8882, PMID: 19591475.

(40) Mebel, A. M.; Georgievskii, Y.; Jasper, A. W.; Klippenstein, S. J. Pressure-dependent rate constants for PAH growth: formation of indene and its conversion to naphthalene. *Faraday Discuss.* **2016**, *195*, 637–670.

(41) Jasper, A. W.; Hansen, N. Hydrogen-assisted isomerizations of fulvene to benzene and of larger cyclic aromatic hydrocarbons. *P. Combust. Inst.* **2013**, *34*, 279 – 287.

(42) Zhao, L.; Kaiser, R. I.; Lu, W.; Xu, B.; Ahmed, M.; Morozov, A. N.; Mebel, A. M.; Howlader, A. H.; Wnuk, S. F. Molecular mass growth through ring expansion in polycyclic aromatic hydrocarbons via radical–radical reactions. *Nat. Commun.* **2019**, *10*.

(43) Mebel, A. M.; Landera, A.; Kaiser, R. I. Formation Mechanisms of Naphthalene and Indene: From the Interstellar Medium to Combustion Flames. *J. Phys. Chem. A* **2017**, *121*, 901–926.

(44) Porfiriev, D. P.; Azyazov, V. N.; Mebel, A. M. Conversion of acenaphthalene to phenalene via methylation: A theoretical study. *Combust. Flame* **2020**, *213*, 302 – 313.

(45) Morita, Y.; Suzuki, S.; Sato, K.; Takui, T. Synthetic organic spin chemistry for structurally well-defined open-shell graphene fragments. *Nat. Chem.* **2011**, *3*, 197–204.

(46) O'Connor, G. D.; Chan, B.; Sanelli, J. A.; Cergol, K. M.; Dryza, V.; Payne, R. J.; Bieske, E. J.; Radom, L.; Schmidt, T. W. Hydrogen-adduction to open-shell graphene fragments: spectroscopy, thermochemistry and astrochemistry. *Chem. Sci.* **2017**, *8*, 1186–1194.

(47) O'Connor, G. D.; Troy, T. P.; Roberts, D. A.; Chalyavi, N.; Fückel, B.; Crossley, M. J.; Nauta, K.; Stanton, J. F.; Schmidt, T. W. Spectroscopy of the Free Phenalenyl Radical. *J. Am. Chem. Soc.* **2011**, *133*, 14554–14557, PMID: 21854045.

(48) Soorkia, S.; Taatjes, C. A.; Osborn, D. L.; Selby, T. M.; Trevitt, A. J.; Wilson, K. R.; Leone, S. R. Direct detection of pyridine formation by the reaction of CH (CD) with pyrrole: a ring expansion reaction. *Phys. Chem. Chem. Phys.* **2010**, *12*, 8750.

(49) Caster, K. L.; Donnellan, Z. N.; Selby, T. M.; Goulay, F. Kinetic Investigations of the CH ($X^2\Pi$) Radical Reaction with Cyclopentadiene. *J. Phys. Chem. A* **2019**, *123*, 5692–5703, PMID: 31194547.

(50) Love, N.; Parthasarathy, R. N.; Gollahalli, S. R. Concentration Measurements of CH and OH Radicals in Laminar Biofuel Flames. *Int. J. Green Energy* **2011**, *8*, 113–120.

(51) Tinaut, F. V.; Reyes, M.; Giménez, B.; Pastor, J. V. Measurements of OH* and CH*

Chemiluminescence in Premixed Flames in a Constant Volume Combustion Bomb under Autoignition Conditions. *Energ. Fuel* **2011**, *25*, 119–129.

(52) Zhang, T.; Guo, Q.; Liang, Q.; Dai, Z.; Yu, G. Distribution Characteristics of OH*, CH*, and C_2* Luminescence in CH_4/O_2 Co-flow Diffusion Flames. *Energ. Fuel* **2012**, *26*, 5503–5508.

(53) Gerin, M., et al. Interstellar CH absorption in the diffuse interstellar medium along the sight-lines to G10.6-0.4 (W31C), W49N, and W51. *Astron. Astrophys.* **2010**, *521*, L16.

(54) Adams, W. S. Some Results with the COUDÉ Spectrograph of the Mount Wilson Observatory. *Astrophys. J.* **1941**, *93*, 11.

(55) Zhou, J.; Fisher, E. R. Surface Reactivity and Energetics of CH Radicals during Plasma Deposition of Hydrogenated Diamondlike Carbon Films. *J. Phys. Chem. B* **2006**, *110*, 21911–21919, PMID: 17064158.

(56) Goulay, F.; Trevitt, A. J.; Meloni, G.; Selby, T. M.; Osborn, D. L.; Taatjes, C. A.; Vereecken, L.; Leone, S. R. Cyclic Versus Linear Isomers Produced by Reaction of the Methylidyne Radical (CH) with Small Unsaturated Hydrocarbons. *J. Am. Chem. Soc.* **2009**, *131*, 993–1005, PMID: 19123915.

(57) Trevitt, A. J.; Prendergast, M. B.; Goulay, F.; Savee, J. D.; Osborn, D. L.; Taatjes, C. A.; Leone, S. R. Product Branching Fractions of the CH + Propene Reaction from Synchrotron Photoionization Mass Spectrometry. *J. Phys. Chem. A* **2013**, *117*, 6450–6457.

(58) Goulay, F.; Trevitt, A. J.; Savee, J. D.; Bouwman, J.; Osborn, D. L.; Taatjes, C. A.; Wilson, K. R.; Leone, S. R. Product Detection of the CH Radical Reaction with Acetaldehyde. *J. Phys. Chem. A* **2012**, *116*, 6091–6106.

(59) Trevitt, A. J.; Goulay, F. Insights into gas-phase reaction mechanisms of small carbon radicals using isomer-resolved product detection. *Phys. Chem. Chem. Phys.* **2016**, *18*, 5867–5882.

(60) Swiderek, P.; Hohlneicher, G. Comment on the Low Lying Singlet States of Acenaphthene. *Ber. Bunsenges. Phys. Chem.* **1991**, *95*, 1683–1684.

(61) Krechkivska, O.; Wilcox, C. M.; Nauta, K.; Kable, S. H.; Schmidt, T. W. Quantum-Induced Symmetry Breaking in the Deuterated Dihydroanthracenyl Radical. *J. Phys. Chem. A* **2019**, *123*, 6711–6719.

(62) Yu, L.; Cullin, D. W.; Williamson, J. M.; Miller, T. A. High resolution laser spectroscopy of asymmetrically deuterated cyclopentadienyl radicals: A study of vibronic degeneracy resolution and Jahn–Teller distortion. *J. Chem. Phys.* **1993**, *98*, 2682–2698.

(63) Reilly, N. J.; Nakajima, M.; Troy, T. P.; Chalyavi, N.; Duncan, K. A.; Nauta, K.; Kable, S. H.; Schmidt, T. W. Spectroscopic Identification of the Resonance-Stabilized cis- and trans-1-Vinylpropargyl Radicals. *J. Am. Chem. Soc.* **2009**, *131*, 13423–13429.